

Comparison of the Degradation Efficiency of Dinitrophenols in Dielectric Barrier Discharge at Gas/Liquid Boundary

Hiroshi OKAWA, Yawara SHIINA, Shin-Ichiro KOJIMA²⁾, Keiko KATAYAMA-HIRAYAMA¹⁾ and Tetsuya AKITSU¹⁾

Happy Science University, 4427-1 Hitotsumatsu-Hei, Chosei, Chiba 299-4325, Japan

¹⁾*University of Yamanashi, 4-3-11 Takeda, Kofu, Yamanashi 400-8511, Japan*

²⁾*Kyushu University, Fukuoka 812-8581, Japan*

(Received 27 December 2020 / Accepted 30 March 2021)

The advanced oxidation of aromatic compounds in aqueous solution has been investigated using a multi-gas, dielectric barrier discharge, and the degradation rate was measured by high performance liquid chromatography (HPLC). In the degradation experiment of 2,5 - DNP, an accelerated degradation pathway was suggested in the transient state, using the molecular orbital calculation of the enhancement of the degradation of oxidation depending on the para-position of nitro-groups. From the nature-friendly technological point of view, a growth of the radish sprout in the hypo-culture was tested after the pH-neutralization of the air-plasma treated water.

© 2021 The Japan Society of Plasma Science and Nuclear Fusion Research

Keywords: dielectric barrier discharge, aromatic compound, dinitrophenol, advanced oxidation, molecular orbital theory, Frontier Electron Theory

DOI: 10.1585/pfr.16.1406070

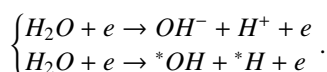
1. Introduction

Dinitrophenol (DNP) is found in the chemical industrial material like antiseptic, dyestuffs, herbicide, and explosive. Warning to the acute and chronic toxicity to human health was addressed in works [1, 2]. Nonthermal, atmospheric-pressure plasma is attracting attentions in the water-treatment for the prevention of the pollution of drinking-water reservoirs by aromatic compounds. The plasma-degradation of the aromatic compound is in several forms: the pulse-streamer discharge and direct current contact glow discharge [3, 4], high intensity UV radiation [5]. In recent works, the decomposition of aromatic compound was reported in multi-gas compact dielectric barrier discharge 2, 6- dibromophenol (DBP) [6] and the experimental discovery of the plasma degradation of 2, 4 - DNP, 2, 5 - DNP, and 3,4 - DNP [7, 8]. New in this work, we discuss the mechanism of the enhanced efficiency of the plasma-degradation in the case of 2, 5 - DNP compared with the case of 2, 4 - DNP on the basis of the molecular orbital theory.

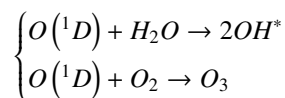
2. Materials and Methods

Lukes *et al.* [9] reported the enhancement of *OH radical production and ozone decomposition in the presence of nitrogen molecules and water vapor, through the following reactions.

Dissociation and ionization generating OH radicals

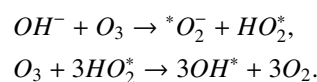


Reactions including excited oxygens

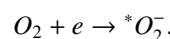


In the air-discharge, the excited state of oxygen is quenched by the humidity, and the ozone production is suppressed.

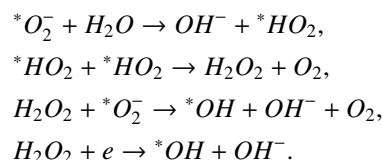
Inhibition of ozone production and enhancement of OH radicals:*



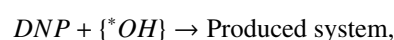
Production of superoxide: Oxygen is the acceptor of electrons and forms:



Production of hydroxyl radicals:

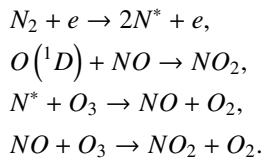


OH* is produced from the dissociation of hydrogen peroxide produced by the excited state of oxygen. Active oxygen radicals are carried in the form of fine bubbles to the liquid phase reaction:

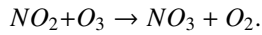


author's e-mail: Hiroshi-okawa@happy-science.university

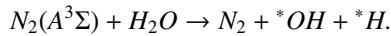
Nitrogen reactions including the quench of $O(^1D)$.



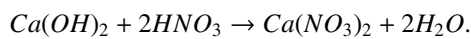
Further oxidation of NO_2 :



Reactions including metastable state of nitrogen molecules



Nitrogen gas contributes to the quench of ozone and the production of oxygen radicals. The liquid waste after the air-plasma treatment shows low-pH due to the accumulation of nitric acid. Demonstration of the nature-friendly technology was tested in the hypo-culture after the pH-neutralization using calcium hydroxide solution.



Calcium hydroxide was selected, considering precipitation of excessive calcium ions using carbon-dioxide gas injection.

In this work, the decomposition of 2,5 - DNP is completed in shorter time compared with the case of 2,4 - DNP. Our speculation stands on the role of the electrophilic reaction by OH to free electron in the transient state shown in Fig. 6 (a) and Appendix A.

In Fig. 1, the dielectric barrier discharge source consists of a quartz tube 3.0 mm and 1.4 mm in outer and inner diameter, and a gas feeder assembled with a Teflon Cajon-type elbow coupler. In the oxidative working gas, W-Re electrode wire is inserted coaxially through a concentric perforation on the wall facing the quartz tube.

The outer part of the quartz tube is submerged in the water solution in a test vial of 100 mL and connected to the ground potential through the capacitive coupling.

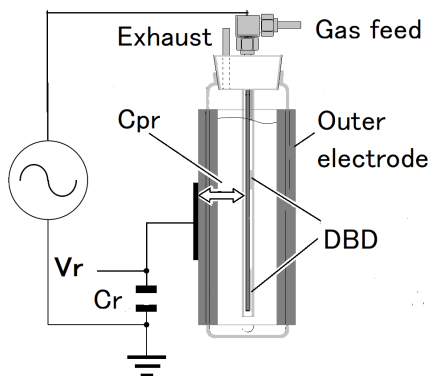


Fig. 1 Multi-gas dielectric barrier discharge in a quartz tube, 3 mm in outer diameter.

Working gas is supplied by a piezo-flow controller. To maintain the reproducible control of the discharge, as in Table 1, the apparatus of the same geometry is used in a series of experiment [6–8]. The discharge is excited with a quasi-sinusoidal high voltage generated by a fly-back transformer-type oscillator (Fig. 2). The discharge current was measured with a current probe and pre-amplifier TCP-312 and TCPA-300, and the terminal voltage was measured with P-3000 voltage probes with TBS 2104 Oscilloscope (Tektronix, USA) Discharge power was estimated averaging the multiplied waveform, comparing with the digitized Q versus V Lissajous figure. The electronic charge Q was measured as the voltage-drop across a ceramic capacitor, $C_r = 4200$ pF connected to the outer electrode surrounding the test vial. The discharge power estimation with the Q versus V Lissajous is summarized in Table 1. A demonstrative example for the Lissajous contour is shown in a leading article [7]. When monitoring capacitor is 4200 pF, one cycle along the contour, 10^{-7} C along the vertical axis multiplied by 5×10^3 V along the horizontal axis is equivalent to 5×10^{-4} J/cycle. The intensity is controlled with the primary DC input of the oscillator. The maximum output is limited by the transition of the discharge mode at 13 V. A comparable result of is shown in Appendix A obtained using different reference capacitor, 10 nF.

Time-elapsed measurement of the concentration was carried out by the high-performance liquid chromatograph

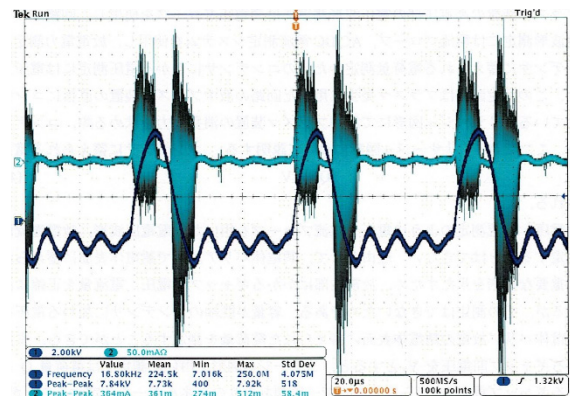


Fig. 2 Typical waveforms. Upper trace: Discharge current. Lower trace: Voltage. Horizontal scale: 20 μs/div [7].

Table 1 Estimation of the discharge power.

Discharge Mode	Parameters	
	Control (V)	Power (W)
Dielectric Barrier Discharge	6.45	3.69
	8.66	6.96
	9.46	9.48
	11.0	12.36
Transfer-type glow discharge	>13	

Frequency: 16.34 - 16.94 kHz

(HPLC). The total organic carbon (TOC) was measured as the amount of carbon-dioxide gas from the incinerated organic materials. HPLC, L-6000 equipped with UV detector, L-4200 (Hitachi Co., Japan) with column X-bridge 4.6, 250 mm (Waters, Japan). TOC measurement was carried out by TOC-LCSH/CSN and auto sampler, ASI-L, (Shimadzu Co., Japan). The reproducibility of the time elapsed measurement and the neutralization process of nitric acid was measured by HPLC Prominence-I LC-2030 Plus (Shimadzu Co., Japan) installed with UV-detector and a reverse mode column: Xbridge C-18, 5 μm.

3. Experimental Results

3.1 Detachment of NO₂ group

In the degradation of DNPs, a remarkable difference was observed between the tendency of two types of DNPs. Figure 3 shows the time elapsed measurement of the concentration of 2,4 - DNP, 2,5 - DNP and catechol in semi-logarithmic scale. The recurrence function is expressed in corresponding exponential functions. The estimated 1/e

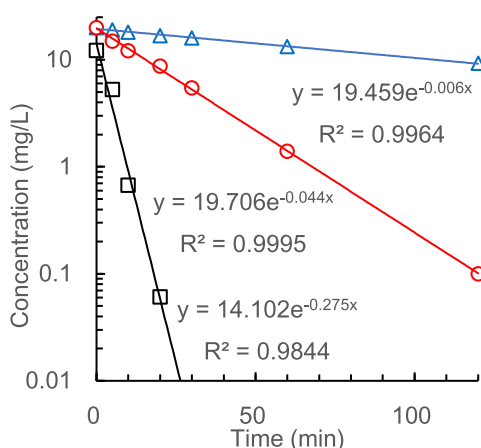


Fig. 3 Comparison of the degradation curve, 2,4 - DNP, 2,5 - DNP and catechol: Semi-logarithmic scale. Control voltage: 10 V. Gas flow: 0.5 L/min. Liquid sample: 50 mL. Triangle symbols: 2, 4 - DNP, circles: 2,5 - DNP; and square symbols: catechol.

Table 2 Estimation of time constant and squared R.

	Time constant (min)	Squared R
2,4- DNP	166.7	0.9964
2,5- DNP	22.7	0.9995
catechol	3.6	0.9844

Table 3 Standard error.

	Average (mg/L)	Standard error*
2,4- DNP	18.1	0.25
2,5-DNP	12.2	0.33
catechol	0.672	0.70

*95 percent confidence interval at 10 min.

time constant and squared R are shown in Table 2. The decomposition time constant of catechol shows wide difference compared with DNPs. Table 3 shows the 95 percent confidence intervals, showing the statistical significance of the separation of each function. Catechol is one of the possible intermediate products, but this peak was not observed in the degradation experiment starting at low density. Plasma degradation of catechol solution, 12.5 mg/L was measured. This peak was not detected except in the extremely high-density case >100 ppm.

4. Discussion

4.1 Difference of the energy level

In the first place, answer to the question why the degradation of 2, 5 - DNP is completed in shorter time. Probably this difference conforms to the difference |LUMO - HOMO| in the energy, where LUMO stands for the lowest unoccupied molecular orbital and HOMO to the highest occupied molecular orbital.

Figure 4 shows the energy diagram for 2, 4 - DNP and the produced system, 4-nitro-catechol and HNO₃. The experimental result conforms the order (Table 4). The energy

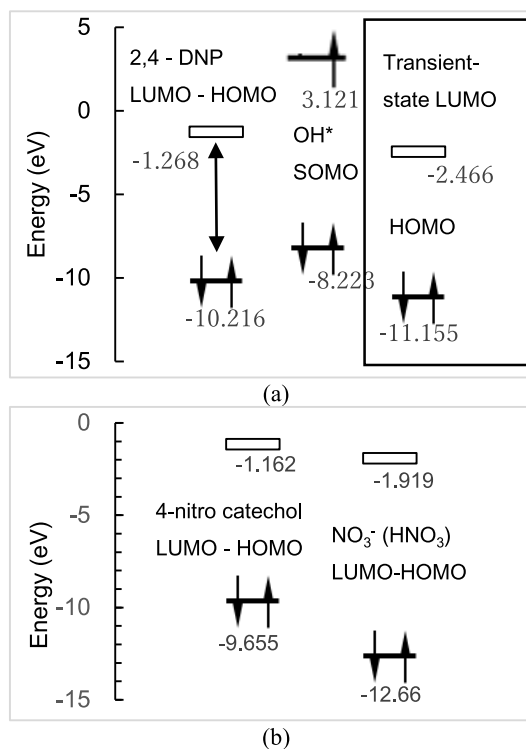


Fig. 4 Energy diagram for 2,4 - DNP, (a) Start and (b) produced system.

Table 4 LUMO - HOMO energy (eV).

	LUMO	HOMO	Difference
2,4 - DNP	-1.268	-10.215	8.947
2,5 - DNP	-2.261	-10.617	8.356

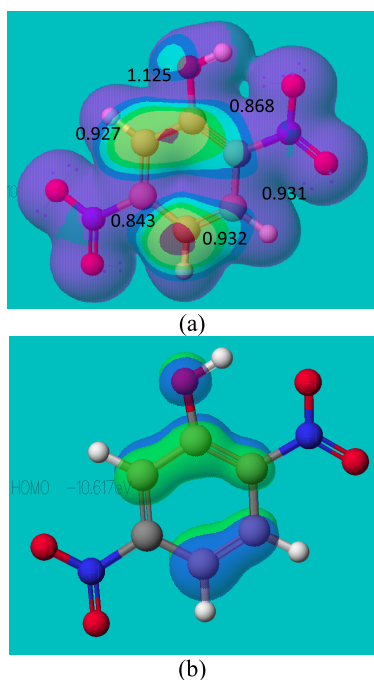


Fig. 5 Electrophilic reaction susceptibility and HOMO surface for 2,5 - DNP (a) Spatial distribution of the electrophilic susceptibility and bond-order: $C(1) - OH$: 1.125; $C(2) - NO_2$: 0.868; $C(3) - H$: 0.931, $C(4) - H$: 0.932; $C(5) - NO_2$: 0.843, $C(5) - H$: 0.927. (b) HOMO surface. HOMO energy: -10.617 eV.

of the Singly Occupied Molecular Orbital (SOMO) of hydroxy radical is 3.121 eV.

The electrophilic reaction occurs at the peak of the electrophilic reaction susceptibility. Two OH systems are connected to carbon atom (1). One of OH systems connected will be released to carbon (2), by the relaxation. Figure 5 shows two peaks of electrophilic reaction susceptibility (a), and the HOMO surface (b).

The electrophilic reaction susceptibility is maximum around the carbon atom connected to phenolic OH.

4.2 Acceleration of electrophilic replacement reaction in the transient state

Figure 6 shows the spatial distribution of the electrophilic reaction susceptibility in the transient states. At the spatial peak of the susceptibility, the phenolic OH and extra OH are connected to adjacent carbon atoms C (1) and C(2). OH and NO_2 -groups are connected to C(2) and C(5).

The bond order in Fig. 6 (a) shows: $C(1) - OH$: 1.114, $C(2) - NO_2$: 0.708, $-OH$: 1.044, $C(3) - H$: 0.935, $C(4) - OH$: 1.114, $C(5) - NO_2$: 0.708, $-OH$: 1.044, $C(6) - H$: 0.935.

NO_2 and OH are attached to carbon (2), in ENOL-type form. As the electrophilic reaction susceptibility is high around the phenolic OH, OH^* is attracted to the electrons of C(1) - C(2) and C(4). When OH and NO_2 attach to C(2), rearrangement of electrons occurs around the benzene ring,

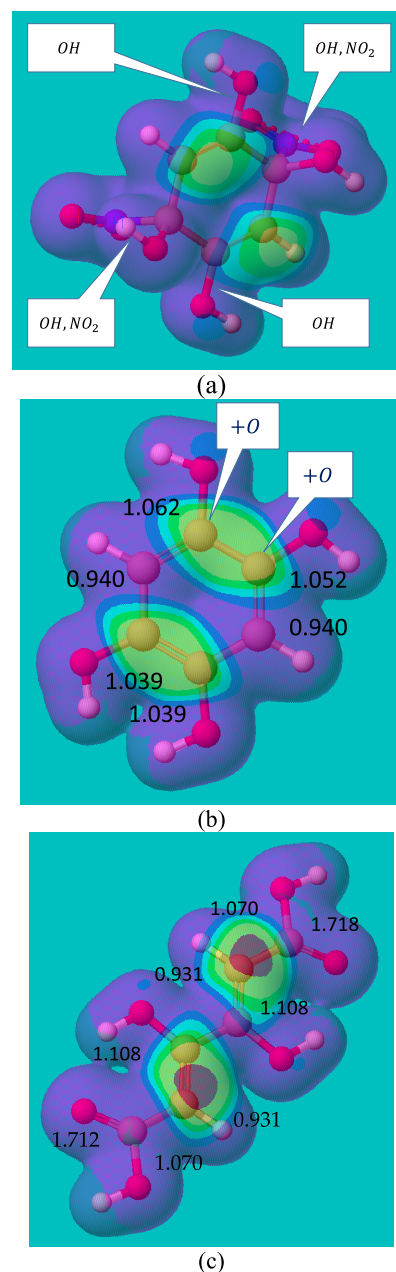


Fig. 6 Electrophilic reaction susceptibility of the transient states of 2,5 - DNP: (a) Before the detachment of NO_2 . Bond orders; $C(1) - OH$: 1.114; $C(2) - NO_2$: 0.708; $C(2) - OH$: 1.044; $C(3) - H$: 0.935; $C(4) - H$: 0.932; $C(5) - NO_2$: 0.838; $C(5) - OH$: 0.937; $C(6) - H$: 0.935. (b) Before and (c) after the cleavage of the aromatic ring [10–13].

and free element appears on C(5). Now, OH is attracted, and NO_2 attaches to C(5). Weaker connections are released in the relaxation and NO_2 is detached.

Cleavage of benzene ring occurs at the region where adjacent two carbon atoms are connected to OH group, C (1) and C (2), where the electron connecting the benzene ring disappears, as in Fig. 6 (b) to (c). Electrophilic reaction occurs in the peak and cleavage of C-C bond in the center. In this way, in 2,5 - DNP, the detachment of NO_2 and the cleavage of benzene ring is accelerated by a free

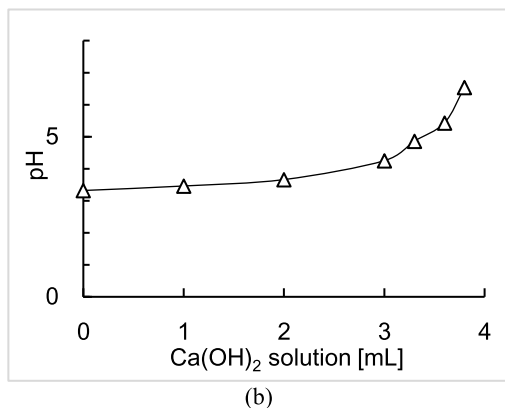
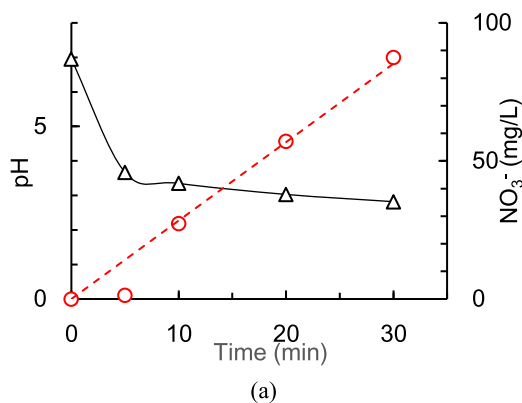


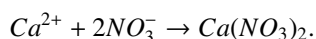
Fig. 7 Air-plasma treated water and pH: (a) Concentration of nitric acid and pH, (b) Neutralization with Ca (OH)₂ solution.

electron which appears at carbon (5) in the transient state. In the case of 2,4 - DNP, the free electron on C(5) may capture an oxygen which will not detach NO₂ connected to C(4), as shown in Appendix A.

4.3 Neutralization and statistical assessment of hypo-culture

4.3.1 Titration of plasma treated water

In Fig. 7, air discharge plasma was injected into 50 mL of distilled water for 30 minutes. The first sample, in 5 minutes, indicated NO₂ and other samples show NO₃. The plasma treated water was produced from distilled water and air-plasma injection, in the same experimental conditions, and pH was adjusted to around 7. The titration was compared with the concentration in HPLC. The HPLC in this experiment was Prominence-I LC2030 Plus with column, Hydrosphere C18, YMC, UV-detector at 210 nm. Buffer: 0.05% phosphoric acid, 1.0 [ml/min]. For example, in the case of 10 minutes of the DBD air plasma injection, Ca(OH)₂ solution in the titration was 3.8 mL. The amount of Ca(OH)₂ 0.5 g/L × 3.8 mL is equal to 25.6436 μmol, and the reaction is



The amount of HNO₃ (62.99564 g/mol) in the titration is



Fig. 8 Growth test of radish-sprout, left: Test group with plasma treated water; right: Control with distilled water.

$$62.9956 \times 51.2872 \times 10^{-6} = 3.2309 \text{ mg.}$$

Relative concentration of HNO₃ is 3.2309/0.09 = 35.899 mg/L. This result corresponds to the estimated value of nitric acid with HPLC: 27.291 mg/L.

The concentration of the nitric acid in the liquid exceeds the hazardous level to aqueous life without the neutralization process (> 30 ppm).

4.3.2 Compatibility test of plasma treated water to plant growth

Radish sprout was cultivated from the seed, and harvested after 2 weeks (Fig. 8). The difference between control (distilled water) and test (neutralized plasma treated water (NPTW)) groups were assessed using 95 percent significance Student's t-test, P- values < 0.05. A typical example for the T-test indicated significant difference between two groups, indicating 1. Average of weight of n = 50 samples was 0.1378 [g] (Control) and 0.1646 [g] (NPTW). Weight as harvested; T-test of 95 percent significance indicated p – value = 0.007814, showing no impediment to the growth, and 2. Average of growth height of n = 50 samples was 21.78 [mm] (Control) and 28.32 [mm] (NPTW). Length as harvested; T-test indicated p – value = 5.596 × 10⁻¹².

Both results indicate the enhancement of the growth of the NPTW group with significance > 95%. Similar tendency was observed in a series of trials. Another example for the Student's T-test and the multiple comparison, Tukey's test is discussed in Appendix C.

5. Conclusions

To provide a method for industrially, efficiently, and simply decomposing benzene derivative having a phenolic hydroxyl group and two nitric systems, a gas/liquid boundary dielectric barrier discharge was tested. Significant difference of the decomposition rate between 2,5 - DNP and 2,4 - DNP were examined using the molecular orbital theory. Our speculation for the experimental result explained considering the acceleration of the attachment of hydroxy radical in the transient states. The nitric acid production in the air plasma may cause strong harmful effect to aqueous life if a large quantity of industrial waste is discharged. The neutralization was tested adding calcium hydroxide solu-

tion. The application in the hydroponic culture indicated no bio-degradation meeting the nature conservation.

Acknowledgments

This research received a fund from Future Science Institute, Tokyo, Japan. The authors express their gratitude to Mr. Kento Nakai, Mr. Kenya Yabu, and Mr. Hiroki Kuroda for their collaboration.

Appendix A. 2, 4 - DNP in the Transient - State

2,4 - DNP Transient state bond order is,

$$C(1) - OH: 0.943, C(2) - NO_2: 0.713,$$

$$C(2) - OH: 1.046, C(3) - H: 0.943,$$

$$C(4) - NO_2: 0.825, C(5) = O: 1.913,$$

$$C(6) - H: 0.932.$$

By the electron's relocation, C(2) and C(3), C(5) and C(6) become double bond and a free electron appears at C(5). C(2) - NO₂ is detached. Then following similar path, the cleavage of the aromatic ring occurs where two adjacent carbon atoms C(1) and C(2) are connected to OH.

Major difference is the free electron on C(5) fails to accelerate the detachment of NO₂ on C(4). The difference may retard the decomposition.

Appendix B. Estimation of the Discharge -Power

Table B1 shows the estimation of the discharge power at different control voltage. The maximum output is limited by the transition of the discharge mode at 19 V.

The DC voltage versus discharge power relation measured using Q versus V Lissajous contour. Terminal voltage was measured with P6015 A high voltage probe and TBS 2104 oscilloscope (Tektronix, USA), reference capacitor 10 nF.

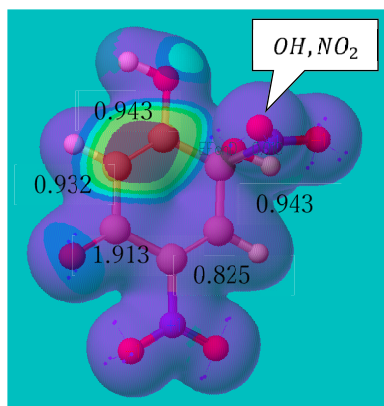


Fig. A1 Electrophilic reaction susceptibility of the transient state of 2,4 - DNP.

Appendix C. Multiple-Comparison: Tukey's Test

First, Student's T-Test, indicated statistically significant difference of the growth height, but fails to deny the equality of the weight. The result indicated, 1. Average of weight was 0.0992 [g] (Control) and 0.1038 [g] (NPTW); T-test indicated p - value = 0.3424. Thus, T-test fails to deny the null-hypothesis: equality of means, and 2. Average of growth height was 33.7004 [mm] (Control) and 41.57012 [mm] (NPTW); T-test indicated p - value = 0.0004241 Null-hypothesis is denied, with 95 % significance.

Multiple comparison, Tukey's method was tested. Three groups of $n = 27$ samples were grown for two weeks with neutralized plasma treated water, as Group 1 - 3, and three groups with distilled water (DW), as Group 4 - 6. Among fifteen possible combinations, statistical difference was observed in the weight between Group - 1 and Group - 5, and Group - 2 and Group - 4, as shown in Table C1, and growth height between Group - 1 and Groups - 4 and 5, as shown in Table C2. In these combinations, p -value is lower than the settled point and the lower limit of the confidence

Table B1 Estimation of the discharge power.

Discharge Mode	Parameters	
	Control (V)	Power (W)
Dielectric Barrier Discharge	6*	1.9
	8	5.88
	10	9.35
	12	12.86
	14	16.95
	16	20.85
18	22.82	
Transfer-type discharge	>19	

Frequency: 16.34 - 16.94 kHz, *6V: 17.90 kHz

Table C1 Comparison of weight ($p < 0.05$).

Statistics	Confidence interval	
	Upper limit	Lower limit
(1,5)	3.25571	0.363288E-01
(2,5)	3.56876	0.381806E-01

Weight (g) of NPTW group

	Group - 1	Group - 2	Group - 3
Average	0.10778	0.109630	0.100370
Variance	0.633333E-3	0.588319E-3	0.649858E-3

Weight (g) of DW group

	Group - 4	Group - 5	Group - 6
Average	0.937037E-1	0.885185E-1	0.102222
Variance	0.439601E-3	0.336182E-3	0.187179E-3

Table C2 Comparison of growth height ($p < 0.05$).

	Statistics	Confidence interval	
		Upper limit	Lower limit
(1,5)	3.22551	16.8136	0.935380
(2,5)	4.63287	20.6857	4.80749

Growth height (mm) of NPTW group

	Group – 1	Group – 2	Group – 3
Average	43.0731	35.4180	37.6629
Variance	126.332	64.7598	118.003

Growth height (mm) of DW group

	Group – 4	Group – 5	Group – 6
Average	34.1986	30.3265	35.3152
Variance	188.440	72.5218	43.1030

interval is positive, showing the growth of NPTW group. Comparison of other combinations failed in the denial of the mean equality null - hypothesis. This result does not conflict to the result of the Student's T-test.

- [1] J. Grundlingh, P. Dargan, M. El-Zanfaly and D.M. Wood, "2,4 – Dinitrophenols (DNP): A Weight Loss Agent with Significant Acute Toxicity and Risk of Death", *Journal of Medical Toxicology*, Sept.; **7(3)**, 205 (2011) Published online 2011, July, 8.
<http://DOI.ORG/10.1007/s13181-011-0162-6>
- [2] Update of Human Health Ambient Water Quality, Criteria: 2,4-Dinitrophenol 51-28-5, United States Environmental Protection Agency, EPA 820-R-15-086, June, 2015.
- [3] J.-Z. Gao, L. Pu, W. Yang, J. Yu and Y. Li, "Oxidative Degradation of Nitrophenols in Aqueous Solution Induced by Plasma with Submerged Glow Discharge Electrolysis", *Plasma Process and Polymer* **171** (2004),
<http://DOI.ORG:10.02/ppap20040012>
- [4] B.R. Locke, M. Sato, P. Sunka, M.R. Hoffmann and J.-S. Chang, "Electrohydraulic Discharge and Nonthermal Plasma for Water Treatment", *Industrial and Engineering Chemistry Research* **45** (3), 882 (2006),
<http://DOI.ORG:10.1021/ie050981u>
- [5] K. Katayama – Hirayama, K. Toda, A. Tauchi, A. Fujioka, T. Akitsu, H. Kaneko and K. Hirayama, "Degradation of dibromo phenols by UV irradiation", *Journal of Environmental Science* **26**, 184 (2014),
[http://DOI.ORG:10.1016/S1001-0742\(13\)60600-2](http://DOI.ORG:10.1016/S1001-0742(13)60600-2)
- [6] S. Kojima, K. Katayama – Hirayama and T. Akitsu, "Degradation of Aqueous 2, 6 – Dibromophenol Solution by In-Liquid Barrier Microplasma", *World Journal of Engineering and Technology* **4**, 423 (2016),
<http://DOI.ORG:10.4236/wjet.2016.43042/>
- [7] H. Okawa, H. Kuroda, K. Katayama – Hirayama, S. Kojima and T. Akitsu, "Plasma-electrolysis of Dinitrophenol in Gas-Liquid Boundary and Interpretation using Molecular Orbital Theory", *World Journal of Engineering and Technology* **7**, 141 (2019), Jan 31, 2019 Online.
<http://DOI.ORG:10.4236/wjet.2019.71010>
- [8] H. Okawa, H. Kuroda, K. Katayama – Hirayama, S. Kojima and T. Akitsu, "Plasma Degradation of Dinitrophenols and Interpretation by the Molecular Orbital Theory", *Plasma Fusion Res.* **14**, 3406071 (2019),
<http://DOI.ORG:10.1585/pfr.14.3406071>
- [9] P. Lukes and B.R. Locke, "Degradation of Substituted Phenols in a Hybrid Gas-Liquid Electrical Discharge Reactor", *Industrial and Engineering Chemistry Research* **44**, 9, 2921 (2005),
<https://DOI.ORG:10.1021/ie0491342>
- [10] K. Fukui, T. Yonezawa and H. Shingu, "A Molecular Orbital Theory of Reactivity in Aromatic Hydrocarbons", *The Journal of Chemical Physics* **20(4)**, 722 (1952),
<http://DOI.ORG:10.1063/1.1700523>
- [11] I. Fleming, *Frontier Orbitals and Organic Chemical Reactions* (Wiley, London, 1978), 24-109, ISBN 0-471-01819-8.
- [12] Biochemical CAChe 6.0 Users Guide, 2003, Fujitsu.
- [13] K. Somekawa, *Molecular Orbital Calculation of Organic Molecules and the Application* (Kyushu University Press, Fukuoka, Japan, 2013) ISBN 978-4-7985-0089-8.